Oscillation mode conversion and energy confinement of acoustically agitated bubbles

Masanori Sato,* Nobunaga Shibuya, Nagaya Okada, and Tonshaku Tou
Honda Electronics Co., Ltd., 20 Oyamazuka, Oiwa-cho, Toyohashi, Aichi 441-3193, Japan

Toshitaka Fujii
Aichi University of Technology, 50-2 Manori, Nishihazama-cho, Gamagori, Aichi 443-0047, Japan
(Received 11 June 2001; revised manuscript received 21 September 2001; published 20 March 2002)

The acoustically agitated bubble oscillation in liquids that is considered to be related to the half-subharmonic acoustic bubble oscillations is discussed in terms of parametric decay instability. At the frequency of about 40 kHz, the half-subharmonic bubble oscillation mode should be a surface bubble oscillation that does not easily emit acoustic waves into water and confines acoustic energy from longitudinal waves. The half-subharmonic bubble oscillation is the dominant mode that leads to parametric decay instability of bubble oscillations.

DOI: 10.1103/PhysRevE.65.046302 PACS number(s): 43.25.+y, 43.35.+d, 03.65.−w

INTRODUCTION

Cavitation is a nonlinear effect of finite-amplitude ultrasonic waves in liquids. The mechanical action of cavitation has been widely used for ultrasonic cleaning, and the localized high temperature and high pressure [1,2] caused by cavitation have recently been utilized to induce chemical reactions for the synthesis of materials. Theories and experiments on cavitation were summarized by Leighton [1].

Nonlinear acoustic effects such as subharmonics have been reported [1,3–15] and analyzed using chaos theory [16–19]. Not only the spherical bubble oscillation mode [1,5–10], but also asymmetric or surface bubble oscillations [1,7–14], in addition to the emission from surface oscillations [8,9], have been discussed. The surface wave or capillary wave (i.e., the standing wave of surface waves) of gas bubble oscillations [1,13] and the destructive action of cavitation [10] have also been discussed. Faraday was the first to report the appearance of the wave of half the exciting frequency [1,20,21]. Neppiras [3] also reported that half of the frequency was obtained from a single air bubble adhering to the hydrophone. The Mathieu differential equation used for analyzing capillary waves of ultrasonic atomization shows a subharmonic instability [21].

In solids, acoustic waves are treated using the phonon concept [22], and a ''three-wave interaction,'' in which one phonon decays into two phonons while fulfilling the frequency- and wave-number matching conditions [23,24], has been recognized. It is also known that one wave decays into two waves, while fulfilling the matching conditions, in the case of parametric decay instability in plasma physics [25] and down conversion in nonlinear optics. Applications of the phonon scheme to acoustic streaming [26–28] and the acoustic radiation pressure [26] of ultrasonic waves in liquid have recently been reported, owing to the simplicity of the mathematical treatment. A subharmonic wave, which is a longitudinal wave mode, is treated using parametric decay [29] with the phonon scheme.

There have been reports that the surface wave is insufficient for the sound source of subharmonic emissions, because the velocity potential decreases rapidly [1,13,14] as one moves away from the bubble. The pressure fields, due to bubbles oscillating asymmetrically, decay with radial distance r as $r^{-(n+1)}$, where $n>1$ [18]; therefore, there is the possibility of acoustic energy confinement in the asymmetric bubble oscillations or surface waves. There is a ''shimmer'' observed on the bubble surface [7], which may indicate that there are surface waves on the bubble surface. Oscillating ripples cause the surface of the bubble to shimmer, as Leighton *et al.* [7] observed by the naked eye. They provided evidence that the oscillating ripples are standing waves, as seen in the photographs [7,10]. Korenfeld and Suvorov [10] noted that all these bubbles, when examined by the naked eye, had twice as many angles as those seen in the photographs. They reported, for example, observation of eight angles (an octagon) by the naked eye, however, only four angles (a square) were seen in the photographs. This indicates that the bubble oscillations are the standing waves of surface waves.

There are two types of parametric decay; spontaneous decay and stimulated parametric decay [30]. Results of a previous study indicate that capillary waves are spontaneously formed on the surface of the bubbles at exactly half the excitation frequency [12]. It has been noted that parametric resonance is insufficient for the deformation of the bubble, because the degree of deformation increases quite rapidly during one period of radial oscillation [11]. Therefore, a nonresonant mechanism for the deformation of the bubble is necessary.

According to the Rayleigh-Plesset equation, there are two types of cavitation modes [1]; stable cavitation and transient cavitation. A transient cavitation bubble expands its radius and finally collapses. Thus, transient cavitation, such as in a cavitation jet, affects the medium mechanically. In contrast, stable cavitation has no collapse phenomenon, so that it appears calm.

In this paper, we propose that an acoustically agitated bubble oscillation is related to half-subharmonic surface bubble oscillation, which does not easily emit acoustic energy into water, i.e., the bubble oscillations are standing surface waves on the bubble surface, or a higher-order mode of bifurcated bubble oscillations. Many analyses of asymmetric

*Email address: msato@honda-el.co.jp

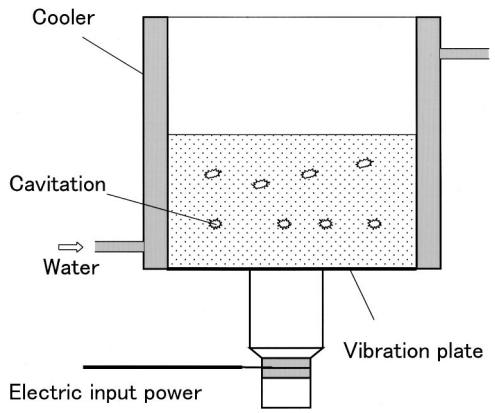

FIG. 1. Experimental apparatus: 100×100×100 mm, 1000 ml capacity.

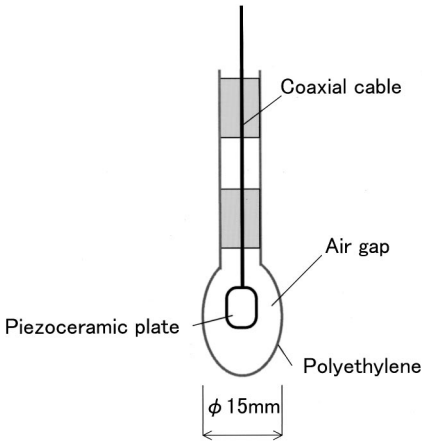

FIG. 2. Structure of hydrophone with an air gap. The air gap (i.e., distance) works as an acoustical filter for the acoustic waves from the point source of bubbles.

bubble oscillations have been performed [1,7–14], however, the bifurcation of asymmetric bubble oscillations has not yet been analyzed from the viewpoint of spontaneous decay using momentum and energy conservation laws. Therefore, we present the experimental results, and propose a method to analyze surface bubble oscillation using parametric decay instability.

I. EXPERIMENT

Figure 1 shows the experimental setup, consisting of a water bath (1000 ml capacity) with a cooling system and an ultrasonic vibrator. The driving frequencies were the higher harmonic oscillation modes of a bolt-fixed Langevin-type vibrator. The vibrator was driven by a power amplifier, the frequency and amplitude were controlled by a signal generator, and the electric input power to the vibrator was measured using an electric power meter.

The half-subharmonics were detected, when acoustically agitated bubbles adhered to the hydrophone, at the driving frequency of about 40 kHz. The subharmonics were strongly depressed when the hydrophone did not directly come into contact with the bubbles. The detection of the half-subharmonics critically depended on the contact between the hydrophone and the bubbles. We detected these data by chance, however, these experimental conditions were not stable, because it was difficult to control the bubble contact with the hydrophone.

In these experiments, we used a hydrophone and an acoustic-filtered piezoceramic hydrophone, so that the longitudinal waves can be distinguished from the surface waves, where the surface oscillating bubbles adhered to the hydrophone. Surface waves from a point source decay very rapidly depending on the distance, therefore, an air gap works as a filter that separates longitudinal waves from surface waves (see Sec. III D). Thus, we introduced an air gap as the acoustical filter for the surface waves. The structure of an air-gapped hydrophone consisted of a piezoceramic plate and a ϕ 15-mm-polyethylene tube (0.2 mm thick), as shown in Fig. 2. The air gap was about 5–7 mm, and the output from the hydrophone was analyzed using a spectrum analyzer after amplification.

In these experiments, separate detection of the oscillations was attempted. The frequency spectrum of an acoustically agitated bubble, which adheres to the hydrophone, is detected directly by comparing the frequency spectrum between the hydrophones with and without an air gap.

II. EXPERIMENTAL RESULTS

Experiments were performed using water, in which a large amount of air was dissolved. The driving frequencies of 43.3 and 140 kHz were used. The depth of the water was 90 mm. Under these conditions, the hydrophone and air-gap hydrophone were set in the water bath. Figure 3 shows the frequency spectrum, where Fig. 3(a) is the result using the no air-gap hydrophone and Fig. 3(b) is the result using the air-gap one. Figure 4 shows the signal intensity level of the frequency spectrum of fundamental (f-) and 1/2 subharmonic ($f/2$-) at the driving frequency $f_0=43.3$ kHz as a function of the electric input power P_0 applied to the vibrators. The various marks in the figure are described in the figure captions, where Fig. 4(a) is the result using the no air-gap hydrophone and Fig. 4(b) is the result using the air-gap one. Figure 4(a) shows that the signal levels of f- and $f/2$- waves depend on the position of the hydrophones and increase according to input power P_0, and $f/2$- waves tend to approach -50 dB when P_0 exceeds 50 W. In the case of the air-gap hydrophone [Fig. 4(b)], the signal level at large P_0 is -100 to -110 dB, which is about 60 dB smaller than the former. The results measured at $f_0=140$ kHz are shown in Fig. 5. From these experimental results, it is observed that the generation of $f/2$ wave increases with an increase in P_0 and a decrease in f_0.

III. DISCUSSION

Here, we discuss the modes of spherical and asymmetric (surface) bubble oscillations, using the quantum mechanical representation [26,28,29] and parametric decay scheme [28,29]. Surface oscillation (i.e., capillary wave) of a solid sphere was calculated by finite-element methods (FEM) as

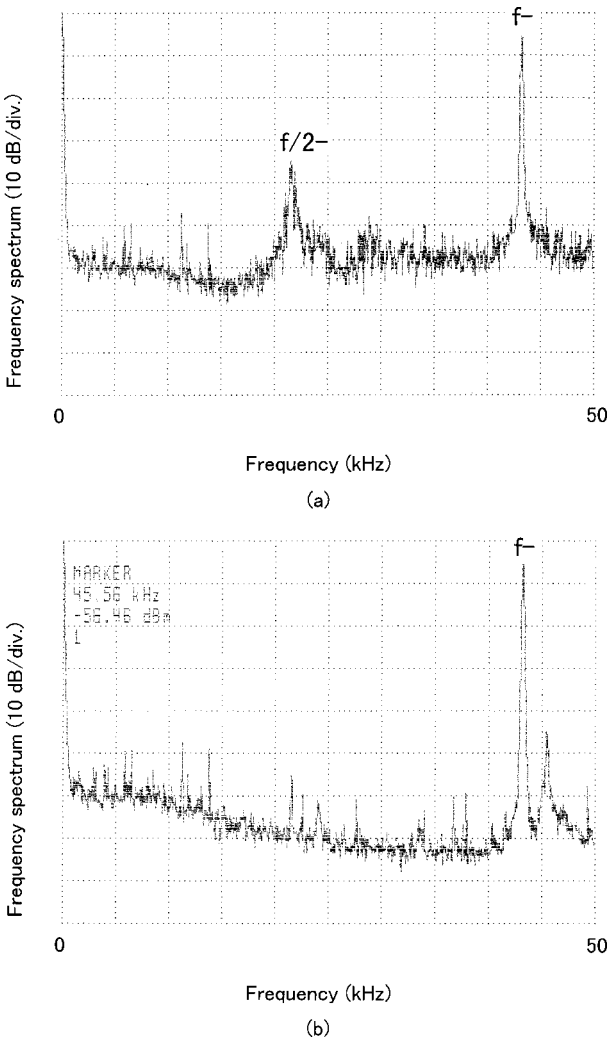

FIG. 3. Frequency spectrum of the fundamental (*f*-) and subharmonic (*f*/2-) waves at the driving frequency of 43.3 kHz, electric input power of 50 W, where (a) hydrophone without an air gap, *f*-: −21.84 dB, *f*/2-: −51.14 dB, (b) hydrophone with an air gap, *f*-: −61.64 dB, *f*/2-: −111.5 dB.

shown in Fig. 6. We think this oscillation mode should be the surface mode of the bubble oscillation. These modes are considered to be half-subharmonic oscillation; at this stage, we cannot calculate the spherical to surface mode conversion nor half-subharmonic oscillation by FEM. We consider that there are two steps in converting spherical bubble oscillation into growing surface bubble oscillation: (1) spherical to surface mode conversion of oscillation, which will occur within one cycle of bubble oscillation [11]; (2) acoustic energy and momentum confinement and accumulation, which will occur in several cycles [31]. These steps can be explained using quantum mechanical representation and energy and momentum conservation laws.

A. Quantum mechanical representation of acoustic wave

Here, we introduce the quantum mechanical representation of an acoustic wave [26–29]. The energy density ε and the momentum density μ are represented by using phonon density n_p,

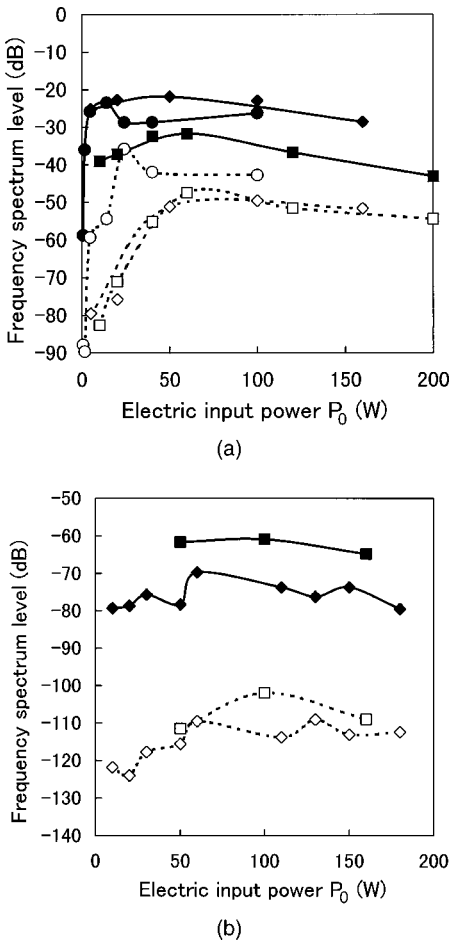

FIG. 4. Signal level of the fundamental (*f*-) (solid symbols) and subharmonic (*f*/2-) (open symbols) waves detected by hydrophone operated at 43.3 kHz as a function of electric input power P_0 (a) hydrophone without an air gap, (b) hydrophone with an air gap. For the hydrophone located 10 mm (from the oscillation plate) ● denotes *f*- and ○ denotes *f*/2-, 40 mm (from the oscillation plate) ◆ denotes *f*- and ◇ denotes *f*/2-, 60 mm (from the oscillation plate) ■ denotes *f*- and □ denotes *f*/2-.

$$\varepsilon = n_p \hbar \omega, \tag{1}$$

$$\mu = n_p \hbar k. \tag{2}$$

Here, $\hbar = h/2\pi$, where h is Planck's constant, $\omega = 2\pi f$ (f is the frequency), and k is the wave number. The representation of Eqs. (1) and (2) is useful for a qualitative understanding of the parametric decay.

Parametric decay is known as three-wave interaction or down conversion, in which one wave decays into two waves, fulfilling the energy and momentum conservation laws, which are represented by Eqs. (3) and (4), respectively,

$$\omega_0 = \omega_1 + \omega_2, \tag{3}$$

$$k_0 = k_1 + k_2. \tag{4}$$

Here, the subscript 0 refers to the original wave, while subscripts 1 and 2 refer to decayed waves.

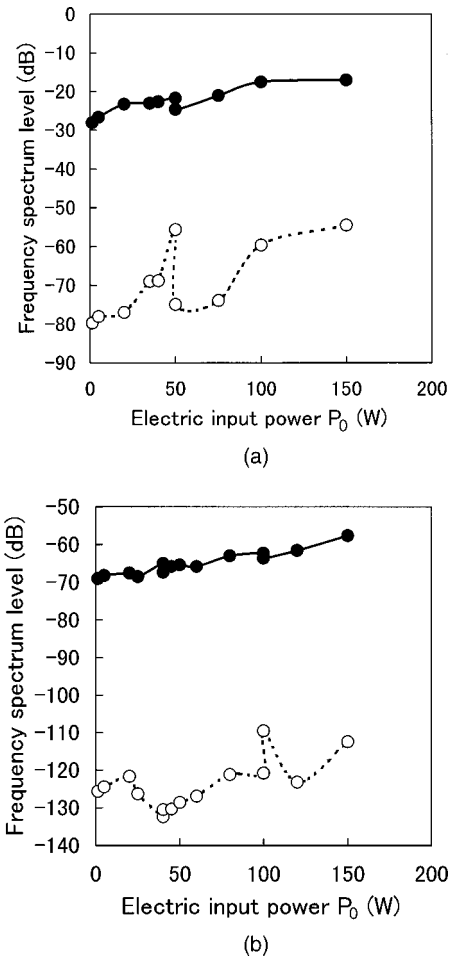

FIG. 5. Signal level of the fundamental (f-) and subharmonic ($f/2$-) waves detected by a hydrophone operated at 140 kHz as a function of electric input power P_0 (a) hydrophone without an air gap, (b) hydrophone with an air gap. For the hydrophone located 10 mm from the oscillation plate ● denote, f and ○ denotes $f/2$.

Parametric resonance is not always a suitable explanation of the parametric decay, because the degree of deformation increases quite rapidly during one period of radial oscillation [11]. The deformation occurs without a resonant process, and the deformation of the bubble oscillation can be explained as an increase in entropy.

B. Mode conversion on the bubble surface

In this section, we propose a simple mechanism of parametric decay, which does not require a parametric resonant process. We consider the parametric decay process as a conversion or deformation process.

First, we qualitatively explain the capillary wave formation mechanism on a flat plane [32] as shown in Fig. 7. The longitudinal waves from the ultrasonic vibrator generate the planar wave fronts, which are parallel to the liquid surface. The longitudinal waves move the surface up and down. However, it is difficult to move a large surface area in phase. Therefore, surface waves (S_+ and S_-) appear on the surface spontaneously, by the rapid deformation of the longitudinal wave (i.e., spontaneous decay).

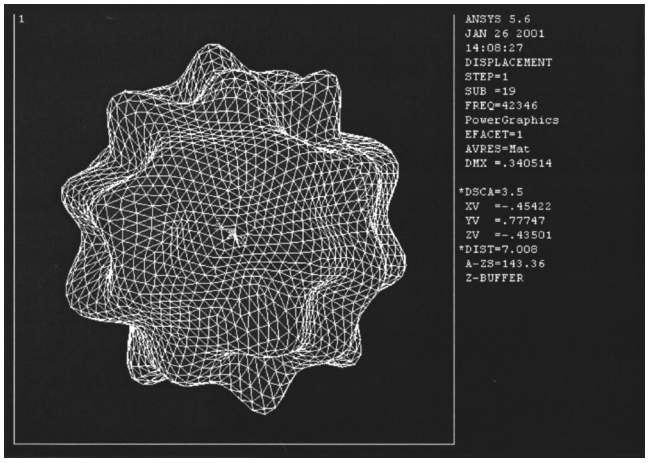

FIG. 6. Surface oscillation of solid sphere shell calculated by FEM.

Capillary waves are generated on the flat plane, and surface bubble oscillation occurs on the bubble surface as capillary waves [33]. We consider it is difficult to oscillate the bubble symmetrically, for example single bubble sonoluminescence occurs at symmetric oscillation, however, an asymmetric oscillation mode does not flash [34]. Therefore, we concluded that it was difficult to obtain a spherical oscillation. There are two types of oscillation modes of the bubble, as shown in Fig. 8, symmetric and surface. The longitudinal wave moves the bubble surface spherically, however, it is difficult to move a bubble surface spherically, resulting in the spontaneous generation of surface bubble oscillations.

C. ω-k diagram

We describe acoustic waves from the viewpoint of momentum and energy; therefore, we introduce the frequency- and wave-number matching conditions, using the ω-k (fre-

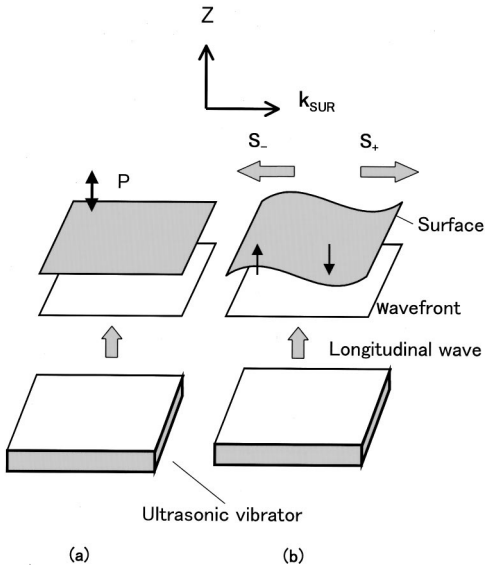

FIG. 7. Surface wave formation by parametric decay: Parametric decay occurs due to an increase in entropy; longitudinal plane waves decay into surface waves spontaneously.

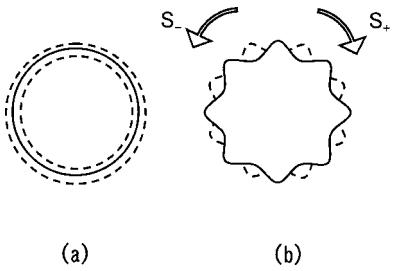

FIG. 8. Asymmetric and spherical bubble oscillations: The parametric decay occurs on the bubble surface, resulting in the generation of capillary waves or asymmetric bifurcated half-subharmonic bubble oscillations. The wave is a standing or traveling surface wave.

quency vs wave number) diagram [25]. Figure 9 shows the coordinates; here, the origin is the center of the bubble, $\mathbf{k}_r$ is the radial wave number direction, and $\mathbf{k}_{\mathrm{SUR}}$ is the wave number along the bubble surface. In the arguments, we use the wave number $\mathbf{k}_{\mathrm{SUR}}$. Figure 10 shows the ω-k diagram of all the waves and oscillations that can exist on the bubble surface. The transversal axis represents the wave number $\mathbf{k}_{\mathrm{SUR}}$, and the vertical axis represents the frequency ω.

Symmetric bubble oscillations are represented as points on the ω axis, because wave-number direction is chosen along the bubble surface; therefore, the symmetric bubble oscillation has an infinite wavelength, i.e., wave number $=0$, and has the frequency ω_0.

Surface acoustic waves are represented as points on the dispersion curves, assuming that the dispersion curves are the same as those for the flat plane surface [20], i.e.,

$$\omega \sim k^{3/2}. \tag{5}$$

Therefore, the ω axis and dispersion curves represent all the oscillations and waves on the bubble surface. Using the ω-k diagram, frequency- and wave-number matching conditions are represented in a parallelogram.

The point P in Fig. 10 is the symmetrical bubble oscillation, driven by the longitudinal wave. If asymmetrical motions occur on the bubble surface, and if these motions fulfil the dispersion relation of the surface waves, parametric decay will occur. If point P decays into further symmetric

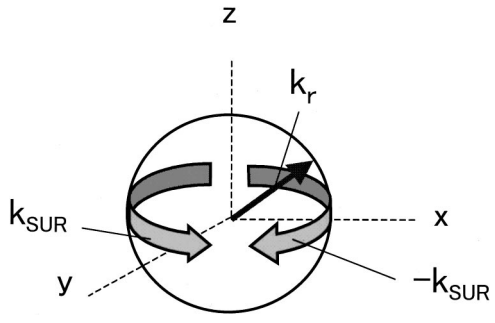

FIG. 9. Coordinates for the analysis of the bubble oscillation: Surface waves do not have radial wave numbers, i.e., radial wave number $\mathbf{k}_r$ is 0, but have wave number $\mathbf{k}_{\mathrm{SUR}}$ that is on the bubble surface.

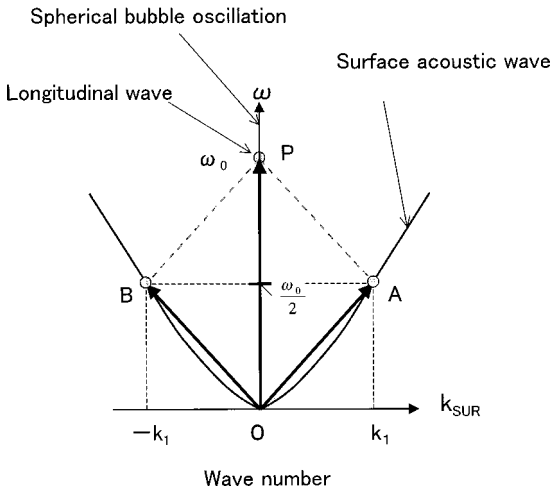

FIG. 10. Frequency vs wave-number (ω-k) diagram of surface wave generation: This diagram represents the parametric decay condition for surface waves on the surface of a liquid. Here, the dispersion curve of the bubble surface is assumed to be similar to that of a flat planar surface.

bubble oscillations, which are represented as the points on the ω axis, these symmetric bubble oscillations will be damped through the emission of the longitudinal waves. Thus, for the confinement of acoustic energy, decayed waves should be nonemission modes, i.e., surface waves on the bubble. Therefore, only the parallelogram *OAPB* can be drawn in this diagram. Here, *OAPB* shows vector summation of $OP(\omega_0,0)=OA(\omega_0/2,k_1)+OB(\omega_0/2,-k_1)$. It means that only this parametric decay pattern has a chance to develop the surface wave and shows a sufficient condition for mode conversion. This is why half of the frequency is generated. The parametric decay condition of *OAPB* shows the wave-number matching condition, which indicates that waves $OA(\omega_0/2,k_1)$ and $OB(\omega_0/2,-k_1)$ propagate in opposite directions. These matching conditions give the half-subharmonic and standing waves. Therefore, equations of the matching conditions (3) and (4) are as follows:

$$\omega_0=\omega_0/2+\omega_0/2, \tag{6}$$

$$0=k_1-k_1. \tag{7}$$

Equation (6) represents half of the frequency (half-subharmonic) condition and Eq. (7) represents the standing wave condition.

D. Acoustic energy and momentum confinment

It is difficult for a surface oscillating bubble to radiate acoustic energy in water, because radiated acoustic pressure amplitude p from the surface waves on the bubble decreases as follows [18],

$$p \propto r^{-(n+1)}. \tag{8}$$

Here, r is the distance from the center of the bubble, and n (>1) is the order of the oscillation mode. Therefore, the acoustic pressure amplitude of the surface waves decreases

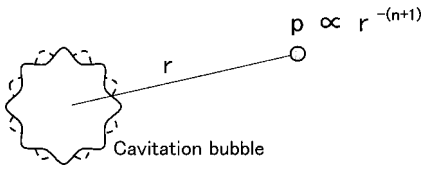

FIG. 11. Distance dependence of the surface acoustic wave pressure amplitude.

very rapidly according to the distance r, as shown in Fig. 11. Hence the energy concentration and confinement occur on the bubble surface.

According to the parametric decay of the bubble oscillations, the energy of the longitudinal waves is transferred to the surface waves, one after another. The surface waves accumulate acoustic energy on the bubble surface, resulting in the breakup of the bubble; this phenomenon is responsible for the instability of parametric decay.

These experimental data are in good agreement with those of previous experiments on the half-subharmonic frequency spectrum [3,6,7,34]. The surface bubble oscillation will be the capillary waves on the bubble surface. We detected separately the longitudinal wave and surface wave of the bubble, by using the no air-gap hydrophone and the air-gap one as described before, where the detection ability of the longitudinal component of the latter is adequately suppressed. This situation is drawn in an intuitive manner in Fig. 12 as the dashed line denotes detection by direct contact and the solid line denotes that by indirect contact through the air gap.

Capillary waves have wave numbers and therefore momentum, producing pressure, which has a possibility of contributing to the breakup of the bubbles. For example, if the bubble radius shrinks, it shortens the wavelength of capillary waves along the bubble surface, resulting in the increase in the wave number (momentum); thus the pressure that makes the bubble radius large is generated on the bubble surface. Therefore, there is a possibility that the capillary waves break up the bubble surface. At this stage, we cannot estimate the contribution of capillary waves that causes the bubbles to breakup.

According to Eqs. (1) and (2), we obtain Eq. (9),

$$\mu = \varepsilon / c. \tag{9}$$

Here, $c = \omega / k$, thus, Eq. (9) indicates that the momentum density depends on the phase velocity; therefore, at equal energy densities the lower the driving frequency, the larger the pressure. This is because at low frequency, the velocity of

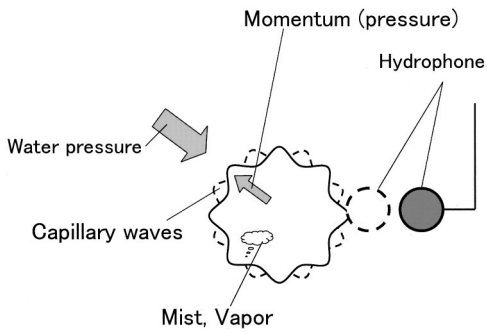

FIG. 12. Surface oscillation mode of acoustically agitated bubble: There is a possibility that the capillary waves function as a wall, which maintains the acoustically agitated bubble surface against the water pressure. Furthermore there is a possibility of the atomization or the vaporization of liquid in the bubble.

the surface wave becomes smaller, as seen from Eq. (5). This fact indicates the possibility that a surface oscillating bubble expands in diameter and finally breaks up at low frequency, while acoustic energy confinement on the bubble surface easily occurs at high frequency. The frequency dependence of surface bubble oscillation is similar to transient and stable cavitation phenomena.

There is a possibility that, in addition to a mechanical reaction, cavitation plays an important role for such chemical reactions as sonochemical luminescence. The frequency dependence of H_2O_2 generation from distilled water [33] can be explained by the mechanism of acoustic energy accumulation on the bubble surface, which is considered to occur more effectively at high frequencies.

CONCLUDING REMARKS

The nonlinear interaction between ultrasonic waves and bubbles is discussed in terms of parametric decay instability. There is a half-subharmonic mode generated from the ultrasonic waves that does not easily emit acoustic energy in liquids. These surface oscillations do not scatter or lose energy, and therefore contribute to the energy accumulation required for the growth of surface bubble oscillation to breakup. We experimentally demonstrated that the surface bubble oscillation has the half-subharmonic surface wave mode with few emissions of acoustic waves into water, resulting in the unstable growth of acoustically agitated bubbles. We consider that the surface bubble oscillation should partially explain the transient cavitation, however, at this stage we cannot show the data of the time scale.

[1] T. G. Leighton, *The Acoustic Bubble* (Academic, San Diego, 1997).
[2] B. P. Barber, C. C. Wu, R. Lfstedt, P. H. Roberts, and J. Putterman, Phys. Rev. Lett. **72**, 1380 (1994).
[3] E. A. Neppiras, J. Acoust. Soc. Am. **46**, 587 (1969).
[4] S. Takahashi, T. Kikuchi, and A. Hasegawa, J. Acoust. Soc. Am. **87**, 2489 (1990).
[5] S. Takahashi and N. Takahashi, Jpn. J. Appl. Phys., Part 1 **35**, 2958 (1996).
[6] A. D. Phelps and T. G. Leighton, J. Acoust. Soc. Am. **99**, 1985 (1996).
[7] T. G. Leighton, R. J. Lingard, A. J. Walton, and J. E. Field, Ultrasonics **29**, 319 (1991).
[8] M. S. Longuet-Higgins, J. Fluid Mech. **201**, 525 (1989).
[9] M. S. Longuet-Higgins, J. Fluid Mech. **201**, 543 (1989).
[10] M. Korenfeld and L. Suvorov, J. Appl. Phys. **15**, 495 (1944).

[11] H. W. Strube, Acustica **25**, 289 (1971).
[12] C. Mullin, Acustica **37**, 64 (1977).
[13] M. Strasberg, J. Acoust. Soc. Am. **25**, 536 (1953).
[14] M. Strasberg, J. Acoust. Soc. Am. **28**, 20 (1956).
[15] W. J. Gallway, J. Acoust. Soc. Am. **26**, 849 (1954).
[16] U. Parlitz, V. Englisch, C. Scheffczyk, and W. Lauterborn, J. Acoust. Soc. Am. **88**, 1061 (1990).
[17] W. Lauterborn and J. Holzfuss, Int. J. Bifurcation Chaos Appl. Sci. Eng. **1**, 13 (1991).
[18] P. Berg, Y. Pomeau, and Ch. Vidal, *L'Ordre dans le Chaos* (Hermann, Paris, 1984).
[19] W. Lauterborn and U. Parlitz, J. Acoust. Soc. Am. **84**, 1975 (1988).
[20] J. W. S. Rayleigh, *The Theory of Sound* (Dover Publications, New York, 1945).
[21] W. Eisenmenger, Acustica **9**, 327 (1959).
[22] I. L. Bajak and M. A. Breazeale, J. Acoust. Soc. Am. **68**, 1245 (1980).
[23] L. H. Taylor and F. R. Rollins, Jr., Phys. Rev. **136**, 591 (1964).
[24] F. R. Rollins, Jr., L. H. Taylor, and P. H. Tood, Jr., Phys. Rev. **136**, 597 (1964).
[25] F. F. Chen, *Introduction to Plasma Physics* (Plenum, New York, 1974), pp. 259–272.
[26] M. Sato and T. Fujii, Phys. Rev. E **64**, 026311 (2001).
[27] M. Sato and T. Fujii, in Proceedings of the 1998 IEEE Ultrasonics Symposium, Sendai, Japan, 1998.
[28] M. Sato, T. Matsuo, and T. Fujii (unpublished).
[29] M. Sato and T. Fujii, Jpn. J. Appl. Phys., Part 1 **36**, 2959 (1997).
[30] J. S. Foster and S. Putterman, Phys. Rev. Lett. **54**, 1810 (1985).
[31] K. S. Suslick, Sci. Am. **260**, 62 (1989).
[32] M. Sato, K. Matsuura, and T. Fujii, J. Chem. Phys. **114**, 2382 (2001).
[33] M. Sato, H. Itoh, and T. Fujii, Ultrasonics **38**, 312 (2000).
[34] Y. Tian, J. Ketterling, and R. E. Apfel, J. Acoust. Soc. Am. **100**, 3976 (1996).